LETTER

BACH2 represses effector programs to stabilize T_{reg}-mediated immune homeostasis

Rahul Roychoudhuri[1]*, Kiyoshi Hirahara[2]†*, Kambiz Mousavi[3]*, David Clever[1], Christopher A. Klebanoff[1], Michael Bonelli[2], Giuseppe Sciumè[2], Hossein Zare[3], Golnaz Vahedi[2], Barbara Dema[4], Zhiya Yu[1], Hui Liu[5], Hayato Takahashi[2], Mahadev Rao[1], Pawel Muranski[1], Joseph G. Crompton[1], George Punkosdy[6], Davide Bedognetti[5], Ena Wang[5], Victoria Hoffmann[7], Juan Rivera[4], Francesco M. Marincola[5,8], Atsushi Nakamura[9,10], Vittorio Sartorelli[3], Yuka Kanno[2], Luca Gattinoni[1], Akihiko Muto[9,10], Kazuhiko Igarashi[9,10], John J. O'Shea[2]* & Nicholas P. Restifo[1,11]*

Through their functional diversification, distinct lineages of CD4^{+} T cells can act to either drive or constrain immune-mediated pathology. Transcription factors are critical in the generation of cellular diversity, and negative regulators antagonistic to alternate fates often act in conjunction with positive regulators to stabilize lineage commitment[1]. Genetic polymorphisms within a single locus encoding the transcription factor BACH2 are associated with numerous autoimmune and allergic diseases including asthma[2], Crohn's disease[3,4], coeliac disease[5], vitiligo[6], multiple sclerosis[7] and type 1 diabetes[8]. Although these associations point to a shared mechanism underlying susceptibility to diverse immune-mediated diseases, a function for BACH2 in the maintenance of immune homeostasis has not been established. Here, by studying mice in which the *Bach2* gene is disrupted, we define BACH2 as a broad regulator of immune activation that stabilizes immunoregulatory capacity while repressing the differentiation programs of multiple effector lineages in CD4^{+} T cells. BACH2 was required for efficient formation of regulatory (T_{reg}) cells and consequently for suppression of lethal inflammation in a manner that was T_{reg}-cell-dependent. Assessment of the genome-wide function of BACH2, however, revealed that it represses genes associated with effector cell differentiation. Consequently, its absence during T_{reg} polarization resulted in inappropriate diversion to effector lineages. In addition, BACH2 constrained full effector differentiation within T_H1, T_H2 and T_H17 cell lineages. These findings identify BACH2 as a key regulator of CD4^{+} T-cell differentiation that prevents inflammatory disease by controlling the balance between tolerance and immunity.

BACH2 is expressed in B cells where it acts as a transcriptional repressor of Blimp-1 (also known as PR domain zinc finger 1) and is critical for somatic hypermutation and class switch recombination[9–11]. Given the association of polymorphisms in the *BACH2* locus with multiple inflammatory diseases in humans, however, we proposed a role for the transcription factor in the prevention of inflammation. To test this hypothesis, we characterized the phenotype of knockout (KO) mice in which the *Bach2* gene had been disrupted[9]. Although pups appeared normal at birth, they developed a progressive wasting disease (Fig. 1a and Supplementary Fig. 1a) that resulted in diminished survival compared to wild-type (WT) littermates (Fig. 1b). Sera from KO mice at 3 months of age contained elevated levels of anti-nuclear and anti-double stranded DNA autoantibodies (Fig. 1c). Gross examination revealed enlargement of the lungs (Fig. 1d and Supplementary Fig. 1b) with highly penetrant histopathological changes (Fig. 1e), including extensive perivascular and alveolar infiltration by lymphocytes

and macrophages (Fig. 1f). Examination of the gut revealed less severe and incompletely penetrant inflammatory pathology of the small intestine and stomach also associated with lymphocytic and macrophage infiltration (Fig. 1g and Supplementary Fig. 2). Consistently, we measured elevated expression of the C-C chemokine receptors CCR4 and CCR9 on splenic CD4^{+} T cells that guide migration to the lung and gut, respectively (Fig. 1h)[12,13]. Accordingly, we found a striking increase in the number of CD4^{+} T cells in the lungs of KO animals, whereas peripheral lymphoid organs contained similar or decreased numbers (Fig. 1i and Supplementary Fig. 3). We also observed increased proportions of effector cells in both the spleen and lungs of KO animals (Supplementary Fig. 4a) and a substantial proportion of CD4^{+} T cells in the lungs expressed the acute activation marker CD69 (Fig. 1j and Supplementary Fig. 4b), a finding indicative of their involvement in the inflammatory process affecting this organ.

CD4^{+} T cells can be characterized into a number of functionally specialized subsets depending upon expression of lineage-specific transcription factors and cytokines[14]. T_H2 cells have a central role in allergic inflammation and airway disease and are characterized by expression of the transcription factor GATA3 and cytokines such as interleukin (IL)-4 and IL-13 (ref. 15). Consistent with the presence of T_H2 inflammation, there were increased proportions of GATA3^{+} CD4^{+} T cells in the spleen and lungs (Fig. 1k and Supplementary Fig. 5) and elevated expression of IL-13 and IL-4 in the spleen, lungs and lymph nodes of KO animals (Fig. 1l and Supplementary Fig. 6a). By contrast, we observed no differences in the frequency of IL-17A^{+} cells in these organs and only a minor increase in interferon (IFN)-γ^{+} cells in the lymph nodes (Supplementary Fig. 6b).

CD4^{+} T cells can function to both drive and constrain immune-mediated pathology. Whereas effector (T_{eff}) cells are often implicated in immune-mediated disease, FOXP3^{+} T_{reg} cells suppress inflammatory reactions and have a non-redundant role in maintaining immune homeostasis[16,17]. Given dysregulated immune reactions in *Bach2*-deficient animals, we measured the expression of *Bach2* messenger RNA (mRNA) in conventional and regulatory CD4^{+} T-cell subsets and their thymic precursors from *Foxp3*[GFP] reporter mice, which express GFP under the control of the endogenous *Foxp3* promoter. *Bach2* mRNA was expressed at high levels in both conventional FOXP3^{−} and FOXP3^{+} (T_{reg}) CD4SP thymocytes in addition to naïve (T_{nai}) and T_{reg} cells in the spleen (Fig. 2a).

Evaluation of conventional thymic maturation in KO animals revealed similar proportions of CD4SP, CD8SP and TCRβ^{+} cells (Supplementary Fig. 7). Given high levels of expression of *Bach2*

[1]Center for Cancer Research, National Cancer Institute, National Institutes of Health (NIH), Bethesda, Maryland 20892, USA. [2]Molecular Immunology and Inflammation Branch, National Institute of Arthritis and Musculoskeletal and Skin Diseases (NIAMS), NIH, Bethesda, Maryland 20892, USA. [3]Laboratory of Muscle Stem Cells and Gene Regulation, NIAMS, NIH, Bethesda, Maryland 20892, USA. [4]Laboratory of Molecular Immunogenetics, NIAMS, NIH, Bethesda, Maryland 20892, USA. [5]Department of Transfusion Medicine, NIH, Bethesda, Maryland 20892, USA. [6]National Institutes of Allergy and Infectious Diseases, NIH, Bethesda, Maryland 20892, USA. [7]Division of Veterinary Resources, NIH, Bethesda, Maryland 20892, USA. [8]Sidra Medical and Research Centre, Doha, Qatar. [9]Department of Biochemistry, Tohoku University Graduate School of Medicine, Sendai 980-8575, Japan. [10]CREST, Japan Science and Technology Agency, Sendai 980-8575, Japan. [11]NIH Center for Regenerative Medicine, NIH, Bethesda, Maryland 20892, USA. †Present address: Department of Advanced Allergology of the Airway, Graduate School of Medicine, Chiba University, Chiba 260-8670, Japan.
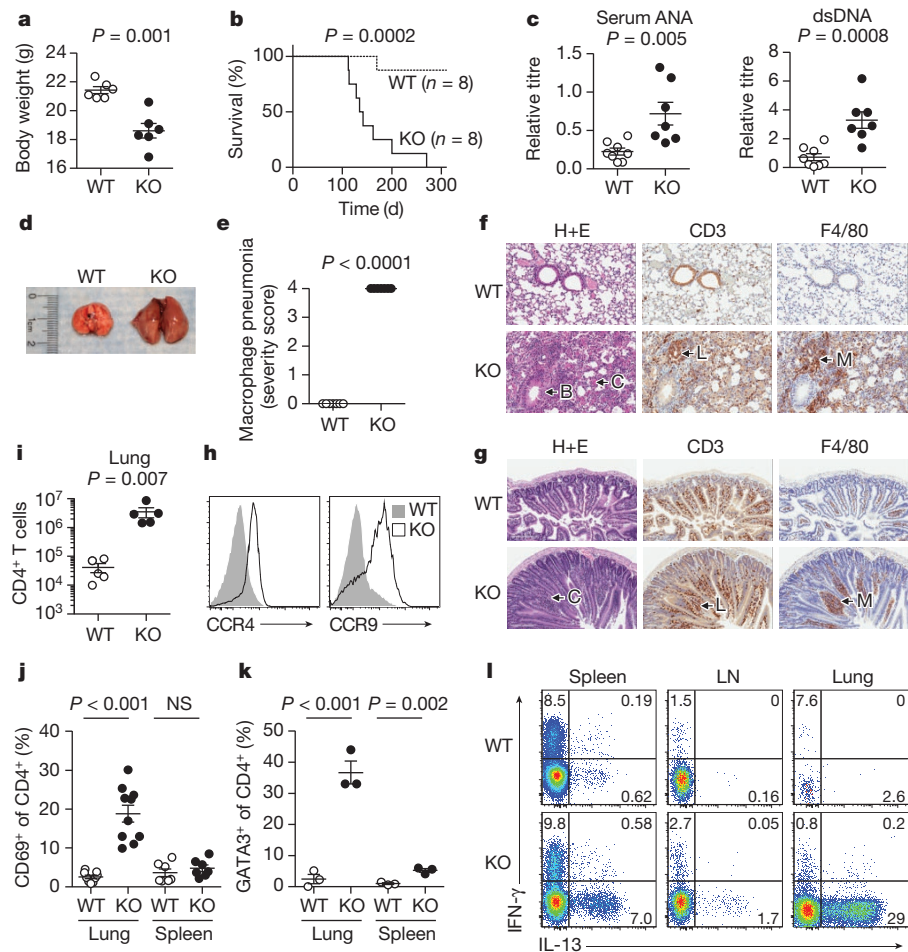*These authors contributed equally to this work.

Figure 1 | Spontaneous lethal inflammation in *Bach2* knockout animals.
a, b, Body weight at 3 months of age (**a**) and survival (**b**) of *Bach2* knockout (KO) and wild-type (WT) littermate females. **c**, Titre of anti-dsDNA antibodies and anti-nuclear antibodies (ANA) in the sera of WT and KO animals. **d**, Gross morphology of lungs from WT and KO mice. **e**, Histopathology scoring of lung tissue from WT and KO mice ($n = 7$ per group). **f**, Haematoxylin and eosin (H+E) and immunohistochemical (IHC) stains of WT and KO lung tissue with hypertrophy of bronchial epithelium (B), eosinophilic crystals (C), perivascular lymphocytic infiltration (L) and macrophage infiltration (M). **g**, H+E and IHC stains of small intestinal tissue lesions with hypertrophic crypts (C), lymphocytic infiltration (L) and macrophage infiltration (M). **h**, Expression of CCR4 and CCR9 on the surface of splenic CD4$^+$ T cells. **i**, Quantification of CD4$^+$ T cells in lungs of WT and KO animals. **j, k**, Percentage of CD4$^+$ T cells expressing CD69 (**j**) and GATA3 (**k**) in lungs and spleen. **l**, Flow cytometry of IFN-γ and IL-13 expression by CD4$^+$ T cells from spleen, lymph nodes (LN) and lungs. Mice were analysed at 3 months of age unless otherwise specified. Data are representative of ≥ 2 independent experiments with ≥ 3 mice per genotype. Error bars, s.e.m.; *P* values (Student's *t*-test).

mRNA in CD4SP thymocytes, however, we wished to determine the cell-intrinsic function of BACH2 in regulating gene transcription within these cells. We reconstituted *Rag1*$^{-/-}$ hosts with equal mixtures of lineage-depleted bone marrow cells (hereafter BM) from congenically distinguishable Ly5.1$^+$ WT and Ly5.1$^-$ KO animals and measured global gene expression in WT and KO CD4SP cells that had developed within the same host (Supplementary Fig. 8 and Supplementary Table 1). Gene set enrichment analysis (GSEA) of this data set (Supplementary Tables 2–6) indicated the loss of genes known to be dependent upon FOXP3 (ref. 2) or directly bound by FOXP3 (Supplementary Fig. 9a)[18]. Consistent with these observations, *Foxp3* mRNA itself showed the greatest fold-reduction in expression amongst all transcripts measured (Fig. 2b and Supplementary Fig. 9b). Consequently, we observed a near complete absence of FOXP3$^+$ cells amongst KO CD4SP thymocytes in WT:KO mixed BM chimaeric animals (Fig. 2c and Supplementary Fig. 10). In animals reconstituted with either KO BM alone (Fig. 2c) or equal mixtures of KO and *FoxP3*^{sf} BM (Supplementary Fig. 11), however, FOXP3$^+$ KO cells were present in both the thymus and spleen but at a lower frequency than when WT cells were transferred. Taken together, these findings indicated a cell-autonomous requirement for BACH2 in the formation of T$_{reg}$ cells in the thymus with an incomplete defect in non-competitive environments.

Whereas a proportion of T$_{reg}$ cells found in peripheral tissues arise in the thymus (thymic T$_{reg}$ or tT$_{reg}$)[16], induced T$_{reg}$ (iT$_{reg}$) cells develop from conventional FOXP3$^-$ CD4$^+$ T cells in extrathymic tissues. To test whether BACH2 was required for efficient formation of iT$_{reg}$ cells, we tracked the fate of naive CD4$^+$ T cells upon transfer into *Rag1*$^{-/-}$ hosts. Although a proportion of WT CD4$^+$ T cells converted into FOXP3$^+$ iT$_{reg}$ cells, significantly fewer KO cells underwent similar conversion (Supplementary Fig. 12). By contrast, KO cells showed similar stability of FOXP3 expression and survival upon transfer into *Rag1*$^{-/-}$ hosts over acute time points (Supplementary Fig. 13). Consistent with *in vivo* data, KO naive CD4$^+$ T cells were markedly impaired in their ability to induce *Foxp3* mRNA and form FOXP3$^+$ iT$_{reg}$ cells upon stimulation in the presence of TGF-β *in vitro* (Fig. 2d, Supplementary Fig. 14). Despite this, KO cells exhibited intact TGF-β and IL-2 signalling (Supplementary Fig. 15). Importantly, defective iT$_{reg}$ induction in KO cells was rescued by reconstitution with *Bach2*-expressing retroviruses (Fig. 2e), confirming that BACH2 is required during induction for the formation of iT$_{reg}$ cells. In addition, *Bach2* overexpression in WT cells enhanced FOXP3 induction under suboptimal polarizing conditions (Supplementary Fig. 16).

Taken together, our results demonstrated a requirement for BACH2 in the efficient generation of both tT$_{reg}$ and iT$_{reg}$ cells. Accordingly,
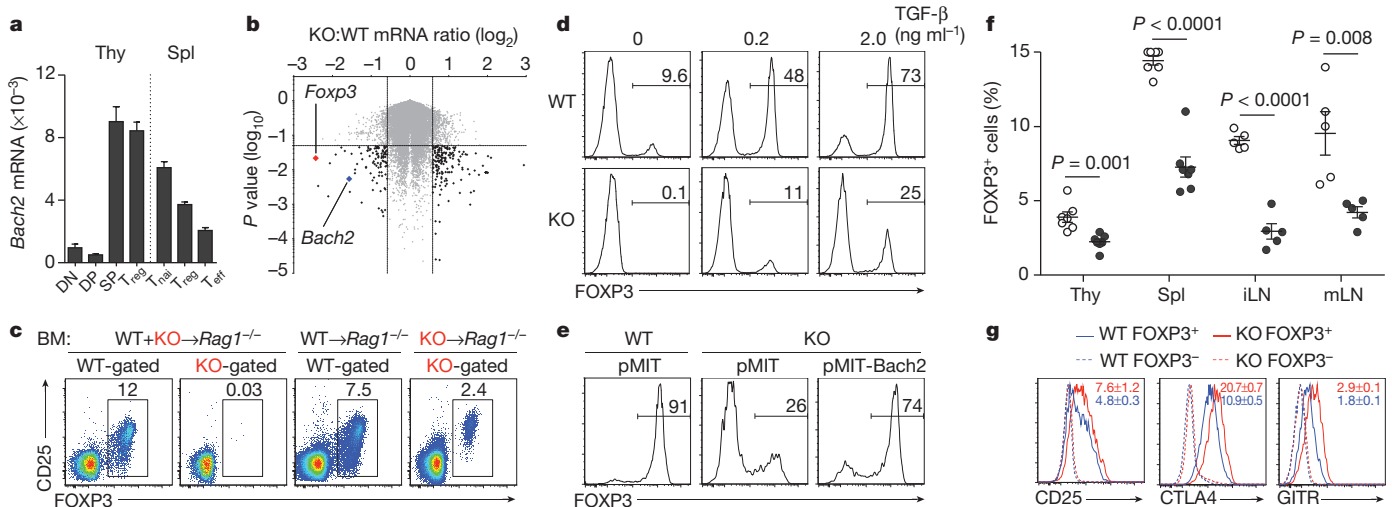
Figure 2 | BACH2 is required for efficient formation of T_reg cells.
a, Expression of *Bach2* mRNA in thymic *Foxp3*$^{GFP-}$ DP and CD4SP (SP), and *Foxp3*$^{GFP+}$ CD4SP T_reg cells and splenic CD4$^+$ *Foxp3*$^{GFP-}$ T_nai and T_eff, and *Foxp3*$^{GFP+}$ T_reg cells isolated from *Foxp3*^{GFP} reporter mice relative to *Actb* mRNA. Thy, thymus; Spl, spleen. **b**, Volcano plot indicating differentially expressed genes in KO compared with WT CD4SP thymocytes from WT:KO mixed BM chimaeric animals. **c**, Intracellular FOXP3 expression in CD4SP thymocytes from mice reconstituted with individual or mixed transfers of WT and KO BM. **d**, FOXP3 expression in WT and KO naive splenic CD4$^+$ T cells stimulated in the presence of indicated amounts of TGF-β *in vitro*. **e**, FOXP3 expression in Thy1.1$^+$ (transduced) WT and KO naive splenic CD4$^+$ T cells stimulated in the presence of 2 ng ml^{-1} TGF-β and transduced with indicated retroviruses. **f**, Ratio of FOXP3$^+$ cells in thymic (gated on CD4SP) and extrathymic tissues (gated on CD3$^+$ CD4$^+$ cells) of 3-month-old WT (open circles) and KO (closed circles) littermates. iLN, inguinal lymph nodes. **g**, Expression of CD25, CTLA4 and GITR on the surface of splenic FOXP3$^+$ and FOXP3$^-$ CD4$^+$ cells from WT and KO mice. Error bars, s.e.m.; *P* values (Student's *t*-test). All data are representative ≥ 2 independent experiments with ≥ 3 mice per genotype (**a–c**, **f**, **g**) or ≥ 4 experiments (**d**, **e**).

analysis of primary and secondary lymphatic tissues from KO mice at 3 months of age revealed a deficiency in T_reg cells resembling that in mice individually reconstituted with KO BM (Fig. 2f). Similar reduction in thymic T_reg cell frequency was observed in neonatal mice before evidence of autoimmune disease (Supplementary Fig. 17). Furthermore, T_reg cell formation was *Bach2* gene-dose dependent because mice heterozygous for the KO allele had reduced frequencies of T_reg cells (Supplementary Fig. 18). Thus, T_reg cells are found at low frequencies in KO mice despite the presence of inflammation in these animals. Characterization of these cells revealed higher levels of expression of T_reg cell suppressive molecules CD25, CTLA4 and GITR (also known as TNFRSF18), the activation marker CD69 and the marker of terminal differentiation, KLRG1 (Fig. 2g and Supplementary Fig. 19; *P* < 0.05)[19]. Consistent with this terminally differentiated phenotype, T_reg cells from *Bach2*-deficient mice failed to prevent colitis in long-term assays despite possessing acute suppressive function (Supplementary Fig. 20a–e)[19].

Because T_reg cells maintain immune homeostasis in an immunodominant fashion, disorders resulting from their deficiency are amenable to rescue by provision of wild-type T_reg cells. To test whether failure to maintain immune homeostasis in the absence of BACH2 was a consequence of defective immunoregulatory capacity, we reconstituted lethally irradiated *Rag1*$^{-/-}$ mice with KO BM in the presence or absence of WT BM. Strikingly, although we observed massive induction of effector differentiation amongst KO CD4$^+$ T cells and mucosal thickening of the large intestine accompanied by infiltration of KO cells when KO BM was transferred independently, these changes were prevented by co-transfer of WT BM (Fig. 3a, b and Supplementary Fig. 21a). Consequently, animals reconstituted with KO BM showed profound weight loss and diminished survival whereas co-transfer of WT BM prevented the induction of disease (Supplementary Fig. 21b, c). The dominant immunoregulatory effect exerted by *Bach2*-sufficient (WT) BM was dependent upon FOXP3 because BM from mice which possess an intact *Bach2* locus but lack functional FOXP3 protein (*Foxp3*^{sf})[20] could not rescue the phenotype induced by KO BM (Fig. 3c). Moreover, the lethal phenotype induced by KO

BM was rescued by transfer of purified splenic CD4$^+$ CD25$^+$ T_reg cells from WT mice. Thus, BACH2 is required for the prevention of lethal autoimmunity through its role in T_reg cell formation.

Taken together, these results demonstrated a non-redundant role for BACH2 in T_reg-mediated immune homeostasis. For transcriptional repression, BACH2 is dependent upon a DNA-binding basic leucine zipper region located near the carboxy terminus of the protein[21].
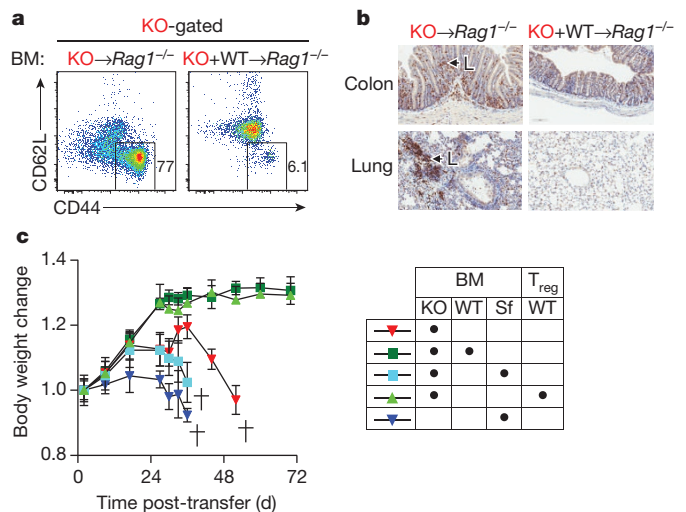

Figure 3 | BACH2 is required for suppression of lethal inflammation in a T_reg-dependent manner. a, CD44 and CD62L expression on splenic CD4$^+$ T cells descended from KO BM 6 weeks following individual or mixed reconstitution of *Rag1*$^{-/-}$ mice with KO and WT BM. **b**, CD3 staining of large intestine and lung tissue from mice 6 weeks following reconstitution with indicated BM. Arrows indicate KO T cells (L). **c**, Mass of mice following individual or mixed reconstitution of *Rag1*$^{-/-}$ animals with BM from Scurfy (*FoxP3*^{sf}), KO or WT mice with or without transfer of 4×10^5 purified splenic CD4$^+$ CD25$^+$ T_reg cells. Data are representative of ≥ 3 independent experiments. Mass measurements were continued until < 3 mice were remaining (**c**). Error bars, s.e.m.

We found that overexpression of a truncation mutant deficient in this region ($Bach2^{\Delta Zip}$) did not complement defective iT_{reg} induction in KO CD4$^+$ T cells (Fig. 4a), implicating its function as a transcriptional regulator in T_{reg} cell formation. To identify genes whose expression is controlled by BACH2, we performed massively parallel RNA sequencing of KO naive CD4$^+$ T cells stimulated under iTreg polarizing conditions. Consistent with its role as a transcriptional repressor, a majority of differentially expressed genes were upregulated in $Bach2$-deficient cells (Supplementary Fig. 22). Strikingly, when we compared these genes with transcripts that were induced upon differentiation of naive cells into effector-lineage T_H1, T_H2 or T_H17 cells, we found that 31.8% (877) of all upregulated genes (2,754) in $Bach2$-deficient cells were effector-lineage-associated genes (Fig. 4b, c).

To test whether BACH2 has a direct role in mediating these transcriptional differences, we measured genome-wide BACH2 binding in iT_{reg} cells by chromatin immunoprecipitation with massively parallel sequencing (ChIP-Seq), validating selected loci by quantitative PCR (Supplementary Fig. 23 and Supplementary Table 7). Remarkably, BACH2 bound 43.6% of all derepressed genes, including 408 derepressed effector lineage-associated genes (Fig. 4b, c). Examples from this group of genes are provided (Fig. 4d and Supplementary Fig. 24a), notably, BACH2 bound and repressed $Prdm1$, which encodes Blimp-1, a transcription factor critical in driving full effector differentiation in CD4$^+$ T cells[22]. BACH2 also repressed genes with

effector-lineage-specific functions such as $Gata3$, $Irf4$ and $Nfil3$, and $Il12rb1$, $Il12rb2$, $Map3k8$ and $Gadd45g$, which have important roles in T_H2 and T_H1 differentiation, respectively[23–27]. Additionally, BACH2 repressed Ahr, which is involved in T_h17 differentiation[28]. Importantly, a number of effector-lineage-associated genes repressed by BACH2 encode proteins that transduce signals antagonistic to T_{reg} cell differentiation itself, including $Il12rb1$, $Il12rb2$ and $Tnfsf4$[29,30]. Repression of $Ccr4$ and $Ccr9$ by BACH2 (Supplementary Fig. 24b) was also of interest since it provides some explanation for the predominance of lung and gut immunopathology in KO animals.

These data indicated that an important aspect of the function of BACH2 is to repress the differentiation programs of multiple effector lineages during iT_{reg} cell development. Accordingly, KO CD4$^+$ T cells stimulated under iT_{reg} conditions aberrantly expressed cytokines associated with effector lineages (Fig. 4e). To test whether BACH2 stabilizes iT_{reg} cell development through repression of effector differentiation, we examined whether blockade of effector cytokines, which play an important role in positive reinforcement of effector cell differentiation, could restore iT_{reg} induction in KO cells. Whereas KO cells stimulated under iT_{reg} conditions preferentially differentiated into FOXP3$^-$ cells expressing T-bet, GATA3 or RORγt, master regulators of the T_H1, T_H2 and T_H17 differentiation programs, respectively (Fig. 4f), addition of neutralizing antibodies against IFN-γ and IL-4 partially reverted this phenotype, preventing aberrant induction of
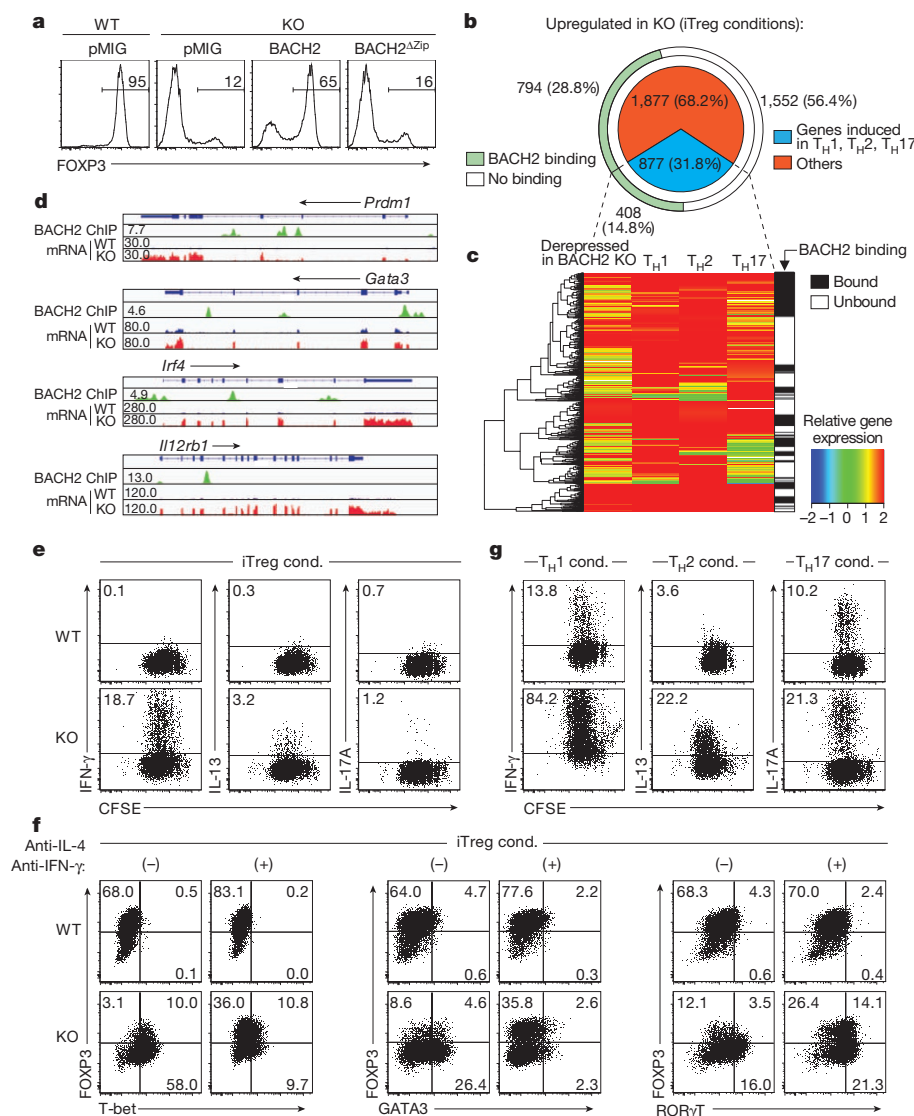

Figure 4 | **BACH2 represses effector programs to stabilize iTreg cell development. a**, FOXP3 expression in GFP$^+$ (transduced) WT and KO naive splenic CD4$^+$ T cells stimulated in the presence of 2 ng ml^{-1} TGF-β and transduced with indicated retroviruses. **b**, Derepressed genes in KO compared with WT naive CD4$^+$ T cells stimulated under iT_{reg} polarizing conditions. Proportion of effector-lineage-associated transcripts (upregulated upon stimulation of naive CD4$^+$ T cells in T_H1, T_H2 or T_H17 conditions respectively (pie chart) and genes that are directly bound by BACH2 in iT_{reg} cells (outer arc) are shown. **c**, Heat map indicating expression of effector-lineage-associated transcripts derepressed in KO cells (iT_{reg} conditions), their expression in wild-type T_H1, T_H2 and T_H17 cells and binding at their respective gene loci by BACH2 (gene-body $\pm$ 2 kb). **d**, Alignments showing binding of BACH2 to selected genes and their mRNA expression in WT and KO cells cultured under iT_{reg} conditions. **e**, Proliferation and effector cytokine expression in CFSE-labelled WT and KO naive CD4$^+$ T cells stimulated under iT_{reg} conditions (cond.) for 3 days. **f**, Transcription factor expression upon stimulation of WT and KO naive CD4$^+$ T cells under iT_{reg} conditions for 3 days in the presence or absence of indicated anti-cytokine neutralizing antibodies. **g**, Proliferation and effector cytokine expression in CFSE-labelled WT and KO naive CD4$^+$ T cells stimulated under indicated polarizing conditions for 3 days. Data are representative of $\geq$ 2 independently repeated experiments (**a**, **e–g**).

T-bet and GATA3 and restoring FOXP3 expression. Interestingly, RORγt expression in KO cells increased in the presence of anti-IFN-γ and anti-IL-4 antibodies, consistent with the recognized ability of IFN-γ and IL-4 to block T_h17 differentiation. Consequently, higher levels of IL-17A were expressed by KO cells under these conditions (Supplementary Fig. 25). These observations raised the possibility that BACH2 might also constrain full effector differentiation amongst conventional T-cell subsets. Strikingly, and consistent with this hypothesis, we observed increased IFN-γ, IL-13 and IL-17A expression when KO naive CD4^{+} cells were stimulated under T_H1, T_H2 and T_H17 conditions, respectively. Thus, additional to its role in T_{reg} cell development, BACH2 limits full effector differentiation in conventional CD4^{+} T cells (Fig. 4g).

During specification of a variety of tissues, negative regulators antagonistic to alternative fates often act in conjunction with positive regulators to stabilize lineage identity[1]. We have identified a function of BACH2 in repressing the differentiation programs of multiple effector lineages in CD4^{+} T cells. By doing so, BACH2 stabilizes the development of T_{reg} cells while limiting full effector differentiation in conventional T cell lineages. Thus, at both a cellular and molecular level, BACH2 functions to constrain immune activation, enabling it to play a critical role in the maintenance of immune homeostasis. These findings help explain the emergence of BACH2 as a key node in human autoimmunity.

METHODS SUMMARY

Experiments were approved by the Institutional Animal Care and Use Committees of the NCI and NIAMS and performed in accordance with NIH guidelines. C57BL/6J, $Rag1^{-/-}$ (B6.129S7-Rag1^{tm1Mom}/J), Ly5.1$^{+/+}$ (B6.SJL-Ptprc^{a}Pepc^b/BoyJ) and Foxp3^{GFP} (B6.Cg-Foxp3^{tm2Tch}/J) mice were purchased from The Jackson Laboratory. Bach2 KO mice, which have been previously described[9], were backcrossed >16 times with C57BL/6 mice.

Full Methods and any associated references are available in the online version of the paper.

1. Rothenberg, E. V., Scripture-Adams, D. D., Competition and collaboration. GATA-3, PU.1, and Notch signaling in early T-cell fate determination. *Semin. Immunol.* **20**, 236–246 (2008).
2. Ferreira, M. A. et al. Identification of *IL6R* and chromosome 11q13.5 as risk loci for asthma. *Lancet* **378**, 1006–1014 (2011).
3. Franke, A. et al. Genome-wide meta-analysis increases to 71 the number of confirmed Crohn's disease susceptibility loci. *Nature Genet.* **42**, 1118–1125 (2010).
4. Christodoulou, K. et al. Next generation exome sequencing of paediatric inflammatory bowel disease patients identifies rare and novel variants in candidate genes. *Gut* http://dx.doi.org/10.1136/gutjnl-2011-301833 (28 April 2012).
5. Dubois, P. C. et al. Multiple common variants for celiac disease influencing immune gene expression. *Nature Genet.* **42**, 295–302 (2010).
6. Jin, Y. et al. Genome-wide association analyses identify 13 new susceptibility loci for generalized vitiligo. *Nature Genet.* **44**, 676–680 (2012).
7. International Multiple Sclerosis Genetics Consortium & The Wellcome Trust Case Control Consortium 2. Genetic risk and a primary role for cell-mediated immune mechanisms in multiple sclerosis. *Nature* **476**, 214–219 (2011).
8. Cooper, J. D. et al. Meta-analysis of genome-wide association study data identifies additional type 1 diabetes risk loci. *Nature Genet.* **40**, 1399–1401 (2008).
9. Muto, A. et al. The transcriptional programme of antibody class switching involves the repressor Bach2. *Nature* **429**, 566–571 (2004).
10. Ochiai, K. et al. Plasmacytic transcription factor Blimp-1 is repressed by Bach2 in B cells. *J. Biol. Chem.* **281**, 38226–38234 (2006).
11. Muto, A. et al. Bach2 represses plasma cell gene regulatory network in B cells to promote antibody class switch. *EMBO J.* **29**, 4048–4061 (2010).
12. Sigmundsdottir, H. & Butcher, E. C. Environmental cues, dendritic cells and the programming of tissue-selective lymphocyte trafficking. *Nature Immunol.* **9**, 981–987 (2008).
13. Lloyd, C. M. et al. CC chemokine receptor (CCR)3/Eotaxin is followed by CCR4/monocyte-derived chemokine in mediating pulmonary T helper lymphocyte type 2 recruitment after serial antigen challenge in vivo. *J. Exp. Med.* **191**, 265–274 (2000).
14. O'Shea, J. J. & Paul, W. E. Mechanisms underlying lineage commitment and plasticity of helper CD4^{+} T cells. *Science* **327**, 1098–1102 (2010).
15. Zhu, J., Yamane, H. & Paul, W. E. Differentiation of effector CD4 T cell populations. *Annu. Rev. Immunol.* **28**, 445–489 (2010).
16. Sakaguchi, S., Fukuma, K., Kuribayashi, K. & Masuda, T. Organ-specific autoimmune diseases induced in mice by elimination of T cell subset. I. Evidence for the active participation of T cells in natural self-tolerance; deficit of a T cell subset as a possible cause of autoimmune disease. *J. Exp. Med.* **161**, 72–87 (1985).
17. Gavin, M. A. et al. Foxp3-dependent programme of regulatory T-cell differentiation. *Nature* **445**, 771–775 (2007).
18. Zheng, Y. et al. Genome-wide analysis of Foxp3 target genes in developing and mature regulatory T cells. *Nature* **445**, 936–940 (2007).
19. Cheng, G. et al. IL-2 receptor signaling is essential for the development of Klrg1^{+} terminally differentiated T regulatory cells. *J. Immunol.* **189**, 1780–1791 (2012).
20. Brunkow, M. E. et al. Disruption of a new forkhead/winged-helix protein, scurfin, results in the fatal lymphoproliferative disorder of the scurfy mouse. *Nature Genet.* **27**, 68–73 (2001).
21. Oyake, T. et al. Bach proteins belong to a novel family of BTB-basic leucine zipper transcription factors that interact with MafK and regulate transcription through the NF-E2 site. *Mol. Cell. Biol.* **16**, 6083–6095 (1996).
22. Crotty, S., Johnston, R. J. & Schoenberger, S. P. Effectors and memories: Bcl-6 and Blimp-1 in T and B lymphocyte differentiation. *Nature Immunol.* **11**, 114–120 (2010).
23. Rengarajan, J. et al. Interferon regulatory factor 4 (IRF4) interacts with NFATc2 to modulate interleukin 4 gene expression. *J. Exp. Med.* **195**, 1003–1012 (2002).
24. Zheng, W. & Flavell, R. A. The transcription factor GATA-3 is necessary and sufficient for Th2 cytokine gene expression in CD4 T cells. *Cell* **89**, 587–596 (1997).
25. Murphy, K. M. et al. Signaling and transcription in T helper development. *Annu. Rev. Immunol.* **18**, 451–494 (2000).
26. Watford, W. T. et al. Tpl2 kinase regulates T cell interferon-γ production and host resistance to *Toxoplasma gondii. J. Exp. Med.* **205**, 2803–2812 (2008).
27. Kashiwada, M., Cassel, S. L., Colgan, J. D. & Rothman, P. B. NFIL3/E4BP4 controls type 2 T helper cell cytokine expression. *EMBO J.* **30**, 2071–2082 (2011).
28. Veldhoen, M. et al. The aryl hydrocarbon receptor links T_H17-cell-mediated autoimmunity to environmental toxins. *Nature* **453**, 106–109 (2008).
29. Xiao, X. et al. OX40 signaling favors the induction of T_H9 cells and airway inflammation. *Nature Immunol.* **13**, 981–990 (2012).
30. Oldenhove, G. et al. Decrease of Foxp3^{+} Treg cell number and acquisition of effector cell phenotype during lethal infection. *Immunity* **31**, 772–786 (2009).

Author Contributions R.R., K.H., J.J.O'S. and N.P.R. wrote the manuscript and designed experiments; R.R., K.H., K.M., D.C., M.B., G.S., Y.K., B.D., Z.Y., H.T. and H.L. carried out experiments; R.R., H.Z., G.V., E.W., V.S., J.J.O'S. and N.P.R. analysed experiments; V.H. performed histopathological evaluations; G.P., A.N., A.M. and K.I. contributed reagents; C.A.K., M.R., P.M., J.G.C., J.R., D.B., A.N., A.M., F.M.M., L.G., V.S. and K.I. edited the manuscript.

Author Information Massively parallel RNA and ChIP sequencing data have been deposited to the Gene Expression Omnibus under the accession number GSE45975. Reprints and permissions information is available at www.nature.com/reprints. The authors declare no competing financial interests. Readers are welcome to comment on the online version of the paper. Correspondence and requests for materials should be addressed to R.R. (roychoudhuri@mail.nih.gov), J.J.O'S. (osheajo@mail.nih.gov) or N.P.R. (restifo@nih.gov).

METHODS

Mice. Experiments were approved by the Institutional Animal Care and Use Committees of the NCI and NIAMS and performed in accordance with NIH guidelines. C57BL/6J, $Rag1^{-/-}$ (B6.129S7-Rag1$^{tm1Mom/J}$), Ly5.1$^{+/+}$ (B6.SJL-Ptprc^{a}Pepc^b/BoyJ) and Foxp3^{GFP} (B6.Cg-Foxp3^{tm2Tch}/J) mice were purchased from The Jackson Laboratory. Bach2 KO mice, which have been previously described[9], were backcrossed >16 times with C57BL/6 mice.

Plasmid DNA and cloning. For the generation of pMSCV-IRES-Bach2-Thy1.1, a fragment of Bach2 cDNA was amplified by PCR from pMSCV-IRES-Bach2-EGFP[1] using the following primers: forward, 5′-GTATTAGCGGCCGCAGACC ATGGACTACAAGGACGACGATGACAAG-3′ and reverse, 5′-GATGAAATC GATCTAGGCATAATCTTTCCTGGGCTGTTCGTCCG-3′ and cloned between the NotI and ClaI sites within the multiple cloning site of pMSCV-IRES-Thy1.1-DEST (pMIT; Addgene 17442). pMIG-Bach2 and pMIG-Bach2$^{\Delta Zip}$ have been described previously[10].

Cell culture. CD4$^+$ T cells from spleens and lymph nodes of 6–8-week-old mice were purified by negative magnetic selection (Miltenyi) followed by sorting of naive CD4$^+$ CD62L^{high} CD44$^-$ CD25$^-$ cells using a FACSAria II sorter (BD). For isolation of T$_{reg}$ cells, CD4$^+$ GFP$^+$ cells were sorted from Foxp3^{GFP} reporter mice or CD4$^+$ CD25^{high} cells were sorted from WT mice. Naive CD4$^+$ T cells were activated with plate-bound anti-CD3 and soluble anti-CD28 (10 μg ml^{-1} each; eBioscience) in media for 3 days either under: Th0 conditions (media alone); Th1 conditions (IL-12 (20 ng ml^{-1}, R&D Systems) and anti-IL-4 neutralizing antibodies (10 μg ml^{-1}, BioXCell)); T$_H$2 conditions (IL-4 (20 ng ml^{-1}, R&D Systems) and anti-IFN-γ neutralizing antibodies (10 μg ml^{-1}, BD Pharmingen)); Th17 conditions (IL-6 (20 ng ml^{-1}, R&D Systems), human TGF-β1 (2 ng ml^{-1}, R&D Systems), anti-IFN-γ neutralizing antibodies (10 μg ml^{-1}) and anti-IL-4 neutralizing antibodies (10 μg ml^{-1})) or iTreg conditions (IL-2 (100 IU ml^{-1}, R&D Systems) and human TGF-β1 (5 ng ml^{-1})). Where indicated, purified naive CD4$^+$ T cells were labelled with carboxyfluorescein succinimidyl ester (CFSE, 1 mM, Molecular Probes) for 8 min at room temperature. The labelling reaction was quenched by washing in FCS.

Retroviral transduction. 20 μg of retroviral plasmid DNA along with 6 μg pCL-Eco plasmid DNA were transfected using 60 μl Lipofectamine 2000 in 3 ml OptiMEM (Invitrogen) for 8 h in antibiotic-free media on Platinum-E ecotropic packaging cells (Cell Biolabs) plated a day prior on poly-D-lysine-coated 10-cm plates (Becton Dickinson) at a concentration of 6×10^6 cells per plate. Media were replaced 8 h after transfection and cells were incubated for a further 48 h. Retroviral supernatants were collected and spun at 2,000g for 2 h at 32 °C onto 24-well non-tissue culture treated plates coated overnight in Retronectin (20 μg ml^{-1}; Takara Bio) and 5 μg ml^{-1} anti-CD3 (2C11) and 5 μg ml^{-1} anti-CD28 (37.51) (eBioscience). Supernatant was discarded and cells were applied to plates 1 day after stimulation in triplicate wells for 24 h in the presence of polarizing cytokines. Following transduction, cells were cultured on fresh anti-CD3 coated plates until analysis at day 5 post-stimulation.

Antibodies and flow cytometry. The following fluorescent dye-conjugated antibodies against surface and intracellular antigens were used: anti-FOXP3 (FJK-16s), anti-IL-13 (eBio13A), anti-IL-17A clone eBio17B7 and anti-GATA3 clone TWAJ (eBioscience); anti-Thy1.1 (OX-7), anti-Ly5.1 (A20), anti-KLRG1 (2F1), anti-B220 (RA3-6B2), anti-NK1.1 (PK136), anti-CTLA4 (UC10-4F10-11), anti-CD4 (RM4-5), anti-CD25 (PC61), anti-CD62L (MEL-14), anti-IFN-γ (Cat 554413), anti-IL-4 (Cat 554435), anti-CD44 (IM7) and anti-CD8a clone 53-6.7 (BD Biosciences); anti-GITR Cat. FAB5241A (R&D Systems) and anti-CD19 clone 6D5 (Biolegend). Cells were incubated with specific antibodies for 30 min on ice in the presence of 2.4G2 monoclonal antibody to block FcγR binding. All samples were acquired with a Canto II flow cytometer (Becton Dickinson) and analysed using FlowJo software (TreeStar). Intranuclear staining for FOXP3 was carried out using the FOXP3 staining kit (eBioscience). To determine cytokine expression, cellular suspensions containing T cells were stimulated in media containing phorbol 12-myristate 13-acetate, ionomycin and brefeldin-A (Leukocyte activation cocktail with Golgiplug; BD biosciences) for 4 h. After stimulation, cells were stained an amine-reactive exclusion-based viability dye (Invitrogen) and with antibodies against cell-surface antigens, fixed and permeabilized followed by intracellular staining with specific anti-cytokine antibodies. Single-cell suspensions from lung tissues were prepared by mechanical disruption (GentleMACS, Miltenyi). Countbright beads were spiked-in for the flow cytometric quantification of absolute cell number (Invitrogen).

Autoantibody enzyme-linked immunosorbent assay (ELISA). For measurement of antinuclear antibodies (ANAs), ELISA assays were performed on mouse serum according to manufacturer's instructions (Alpha Diagnostic International). For the measurement of anti-dsDNA autoantibodies, dsDNA-coated plates (Calbiotech) were incubated with serum samples and anti-dsDNA titres were evaluated using a horseradish peroxidase-conjugated anti-mouse antibody (IgG, IgM, IgA) (Alpha Diagnostic International).

Quantitative reverse-transcription polymerase chain reaction (qRT–PCR). Cells were sorted or transferred into RNALater solution (Ambion) and stored at −80 °C. Total RNA from pelleted cells was isolated using the RNeasy Plus mini kit (Qiagen). First-strand cDNA synthesis was performed using random priming with the high-capacity cDNA synthesis kit (Applied Biosystems) in the presence of SuperaseIn RNase inhibitor (Ambion). cDNA was used as a template for quantitative PCR reactions using the following Taqman primer-probes (Applied Biosystems): Actb (mm00607939_s1), Bach2 (mm00464379_m1) and Foxp3 (mm00475162_m1). Reactions were performed using Fast Universal PCR Mastermix (Applied Biosystems) according to the manufacturer's instructions and thermocycled in quadruplicate 10 μl reactions in 384-well plates. Signals in the FAM channel were normalized to ROX intensity, and C_t values were calculated using automatically determined threshold values using SDS software (Applied Biosystems).

Bone marrow chimaeras and T$_{reg}$ cell rescue experiments. For bone marrow reconstitution experiments, $Rag1^{-/-}$ mice were administered 1,000 Gy total-body γ-radiation from a ^{137}Cs source before intravenous injection of BM cells depleted of mature lineages from single-cell bone-marrow preparations using antibody-coupled magnetic beads (Miltenyi). Bone marrow from 6–10-week-old donor mice were used except with Scurfy mice where 12 day old pups were used as donors. Where indicated, 4×10^5 fluorescence-activated cell sorting (FACS)-purified CD4$^+$ CD25$^+$ T cells were transferred intravenously into mice 1 day after transfer of bone marrow cells.

In vivo iT$_{reg}$ induction. $Rag1^{-/-}$ mice were injected intravenously with 4×10^5 CD4$^+$ CD25$^-$ CD45RB^{high} cells from wild-type or Bach2-deficient mice. On day 21 to 23, cells were isolated and analysed for FOXP3 expression.

In vitro suppression assay. Varying numbers of WT and KO CD4$^+$ CD25$^+$ T$_{reg}$ cells were cultured in 96-well round-bottom plates with 5×10^4 CFSE-labelled naive CD4$^+$ CD62L$^+$ CD44^{low} responder (T$_{resp}$) cells along with 1×10^4 CD11c$^+$ dendritic cells used as antigen-presenting cells, isolated by immunomagnetic selection (Miltenyi). Cells were stimulated with 1 μg ml^{-1} anti-CD3 antibody (BD Biosciences) for 72 h at 37 °C and 5% CO$_2$. T$_{resp}$ cell proliferation was measured by flow cytometry.

In vivo suppression assay. In vivo suppression assays were done as previously described[31]. Briefly, $Rag2^{-/-}$ mice were injected intravenously with 1×10^5 CFSE-labelled naive CD4$^+$ CD25$^-$ CD45Rb^{hi} (T$_{resp}$) cells from CD45.1 mice with or without 1×10^5 wild type or BACH2-deficient CD4$^+$ Foxp3^{GFP+} T$_{reg}$ cells. Mice were analysed on day seven for T$_{resp}$ cell proliferation by flow cytometry.

Transfer colitis model. The transfer colitis model has been described previously[32]. Briefly, $Rag1^{-/-}$ mice were injected intravenously with 4×10^5 FACS-sorted naive CD4$^+$ CD25$^-$ CD45RB^{high} cells from CD45.1$^+$ mice with or without 1×10^5 WT or KO CD4$^+$ CD25^{high} T$_{reg}$ cells. Mice were monitored weekly for weight loss and signs of disease, and killed at week 6. Sections of the proximal, mid-, and distal colon were fixed in buffered 10% formalin and stained with haematoxylin and eosin (H&E).

RNA sequencing. RNA sequencing was performed and analysed as described previously[33]. Total RNA was prepared from approximately 1 million cells by using mirVana miRNA Isolation Kit (AM1560, ABI). 200 ng of total RNA was subsequently used to prepare RNA-seq libraries by using TruSeq SRRNA sample prep kit (FC-122-1001, Illumina) according to the manufacturer's instructions. The libraries were sequenced for 50 cycles (single read) using a HiSeq 2000 sequencer (Illumina). Sequence reads from each cDNA library were mapped onto the mouse genome build mm9 by using Tophat, and the mappable data were then processed by Cufflinks[34]. The obtained data were normalized based on RPKM (reads per kilobase exon model per million mapped reads). To find differentially regulated genes, we used a 1.5-fold change difference between genotypes and a fourfold change difference between different lineages.

Chromatin immunoprecipitation. T cells were chemically crosslinked and sonicated to generate fragmented genomic DNA. Chromatin immunoprecipitation was performed using an anti-BACH2 antibody (N-2; Tohoku University). For sequencing of immunoprecipitated DNA, DNA fragments were blunt-end ligated to the Illumina adaptors, amplified, and sequenced by using the Hi-Seq 2000 sequencer (Illumina). Sequence reads of 50 base pairs were obtained by using the Illumina Analysis Pipeline. All reads were mapped to the mouse genome (mm9), and only uniquely matching reads were retained. After removal of redundant reads, enriched peaks were called using ChIP-Seq analysis tool MACS[35]. Around 20,000 peaks were detected at a P-value level of less than 1×10^{-4} and false discovery rate of less than 5%. Peaks in ±2 kb vicinity of gene bodies were assigned to genes to identify the bound target genes. For PCR-based confirmation of BACH2 binding, chromatin immunoprecipitation was performed as described above, and qPCR reactions were carried out on input and immunoprecipitated

DNA using the Power SYBR Green kit (Applied Biosystems) and primers as specified in Supplementary Table 7.

Microarray analysis. 100 ng of total RNA extracted as previously described was amplified using Ovation Pico WTA System V2 (NuGEN) according to the manufacturer's instructions. Briefly, first-strand cDNA was synthesized using the SPIA tagged random and oligo dT primer mix in 10 μl reactions after denaturation and incubated at 65 °C for 2 min and priming at 4 °C followed by extension at 25 °C for 30 min, 42 °C for 15 min and 77 °C for 15 min. Second strand cDNA synthesis of fragmented RNA was performed using DNA polymerase at 4 °C for 1 min, 25 °C for 10 min, 50 °C for 30 min and 80 °C for 20 min. 5′ double stranded cDNA was used as the template for isothermal single-strand cDNA amplification following a cycle of DNA/RNA primer binding, DNA replication, strand displacement and RNA cleavage at 4 °C for 1 min, 47 °C for 75 min and 95 °C for 5 min in total 100 μl reaction. Samples were fragmentated and biotinylated using the Encore Biotin Module (NuGEN) according to the manufacturer's instructions. Biotinylated cDNA was then hybridized to Mouse Gene 1.0 ST arrays (Affymetrix) overnight at 45 °C and stained on a Genechip Fluidics Station 450 (Affymetrix), according to the respective manufacturers' instructions. Arrays were scanned on a GeneChip Scanner 3000 7G (Affymetrix). Global gene expression profiles rank ordered by relative fold-change values were analysed by using Gene set enrichment analysis software (Broad Institute, MIT). P values were calculated using Student's t-test using Partek Genomic Suite after Robust Multiarray Average normalization.

Statistical analysis. Student's t-test was used unless otherwise specified to calculate statistical significance of the difference in mean values and P values are provided. For calculation of statistical significance of differences in clinical histopathology scores, the Wilcoxon rank-sum test was used.

31. Pesu, M. et al. T-cell-expressed proprotein convertase furin is essential for maintenance of peripheral immune tolerance. Nature **455,** 246–250 (2008).
32. Powrie, F., Carlino, J., Leach, M. W., Mauze, S. & Coffman, R. L. A critical role for transforming growth factor-β but not interleukin 4 in the suppression of T helper type 1-mediated colitis by CD45RB^low CD4^+ T cells. J. Exp. Med. **183,** 2669–2674 (1996).
33. Vahedi, G. et al. STATs shape the active enhancer landscape of T cell populations. Cell **151,** 981–993 (2012).
34. Trapnell, C. et al. Transcript assembly and quantification by RNA-Seq reveals unannotated transcripts and isoform switching during cell differentiation. Nature Biotechnol. **28,** 511–515 (2010).
35. Zhang, Y. et al. Model-based analysis of ChIP-Seq (MACS). Genome Biol. **9,** R137 (2008).